ICIC Express Letters
Volume **12**, Number **3**, March **2018**
 ISSN 1881-803X
pp. **277–285**

NUMERICAL SIMULATION OF ATOMIZATION CHARACTERISTICS OF SWIRL NOZZLE

Dianrong Gao[1,*], Yanan Sun[1] and Guangtong Zhang[2]

[1]College of Mechanical Engineering
Yanshan University
No. 438, Hebei Ave., Qinhuangdao 066004, P. R. China
[*]Corresponding author: gaodr@ysu.edu.cn

[2]Beijing Shougang International Engineering Technology Co., Ltd.
No. 60, Shijingshan Street, Shijingshan Dist., Beijing 100043, P. R. China

Received August 2017; accepted November 2017

Abstract. *Compared with other forms of nozzle atomizer, the geometry of the swirl nozzle atomizer is relatively simple, and it has good atomization performance under the premise of saving energy. Based on the theory of hydrodynamics, the simulation software FLUENT is used to simulate the atomization characteristics of swirl nozzle, so as to obtain the relationship between the atomization performance parameters and the working pressure. Simulation results show that with the increase in water pressure, nozzle spray range decreased first and then increased. Atomization angle and the average diameter of droplet gradually decreased. And 0.8 MPa is obtained as the optimum working water pressure for obtaining a good atomizing effect.*
Keywords: Swirl nozzle, Numerical simulation, Atomization characteristics, Water pressure, Droplet diameter

1. **Introduction.** As the fog and haze phenomenon frequently occurs in some parts of the country, the health of residents is seriously affected and an important factor which leads to this phenomenon is respirable particulate matter. At present, wet dust is the main method of managing haze. The nozzle is an important component of wet dust removal equipment and the performance of dust removal depends directly on the atomization capacity of the nozzle. Swirl nozzle nebulizer's geometry is relatively simple. In the premise of saving energy with good atomization performance, it is widely used in environmental protection and other industries.

In recent years, many experts and scholars at home and abroad researched the swirl nozzle from many aspects and made great progress. Ma and Kou found that under the condition that the peak pressure of water pressure was lower than 1 MPa, it could achieve better dust removal performance through improving the water pressure and reducing the nozzle diameter [1]. Ding verified the correctness of the theoretical analysis by simulation and experiment through analyzing and optimizing [2]. Li et al. analyzed the structure of the nozzle core, working pressure and the diameter of droplet, made a variety of combined parameter nozzles, and quantified the influence of different structures on nozzle atomization [3]. Zhang et al. simulated the swirl nozzle by FLUENT, obtained the same result as the experiment, and verified the correctness of the simulation [4]. Yang et al. established a two-dimensional model of the flow field of the conical nozzle and simulated the numerical simulation using the turbulence model through FLUENT. The results show that the atomization performance of the nozzle is the best when the nozzle length and diameter ratio are 2-3 [5]. Ding et al. simulated the dust performance of the nozzle and found that its dust removal efficiency increased with the pressure increasing [6]. Sun analyzed the droplet velocity and droplet diameter in a certain cross-section [7]. Xu et al. used the

DPM model in FLUENT to simulate the operation of the nozzle and proposed the influencing factors of fluid properties mainly including droplet velocity, diameter, density and volume fraction of droplets [8]. Chatterjee et al. used the turbulence model in FLUENT to simulate the nozzle and use the multiphase flow model to simulate the jet transient. The experiment was carried out to simulate the droplet diffusion of the nozzle [9]. Paine et al. used the DPM model in FLUENT to simulate the droplet dropping of swirl nozzles and the distribution range of droplet diameter and droplet velocity [10].

The main directions and methods of the study on the atomization characteristics of swirl nozzles at present are mainly to analyze and optimize the atomization performance of the nozzles by means of experiment or simulation respectively. However, the numerical simulation of nozzle atomization generally focuses on the analysis of the continuous phase of the nozzle. In this paper, the method of discrete phase numerical simulation is used to analyze and optimize the atomization performance of droplet diameter and velocity.

2. **Model Structure and Working Principle of Swirl Nozzle Atomizer.** Figure 1 shows the physical diagram of the swirl nozzle. Because the swirl nozzle internal body diameter is small and precise, the physical diagram is cut along its axis. Figure 2 shows the cut picture of the swirl nozzle. Through the measurement, the relevant model of the swirl nozzle is established by SolidWorks. Figure 3 shows a three-dimensional model of the rotary core. Figure 4 shows an assembly diagram of the whole assembly.

FIGURE 1. Physical nozzle

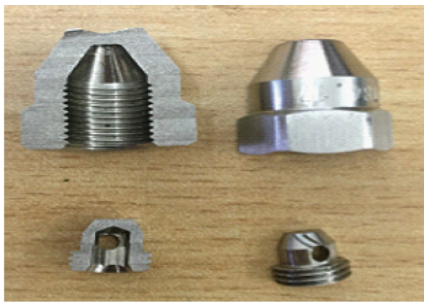

FIGURE 2. Cut nozzle

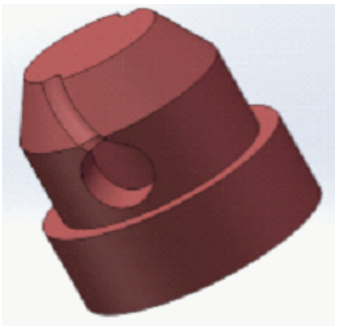

FIGURE 3. Nozzle core

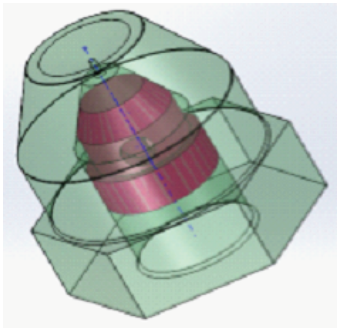

FIGURE 4. Nozzle assembly

Figure 5 shows a cross-sectional view of the swirl nozzle model. The high velocity fluid flows through the swirl nozzle cavity and enters the swirl chamber through the radial holes on both sides of the rotary shaft and is finally ejected from the nozzle outlet. In this process, the fluid formed the liquid film in the centrifugal force, the surface force and the role of air resistance. Then, under the combined action of inertial force and surface force, the liquid film is crushed to form filamentous filaments, and under the action of unbalanced internal and external forces, the formation of droplets continues to be broken, and thus enters a stable atomization state.

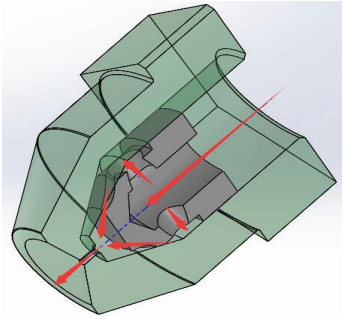

FIGURE 5. Profile of nozzle

3. **Establishment of Nozzle Flow Field Model and Meshing.** The process of simulating the swirl nozzles is mainly about that water enters the nozzle and then ejects into air to atomize. Therefore, it is necessary to establish the flow field model. The three-dimensional model of the swirl nozzle shape is built through SolidWorks and imported into the grid division software Gambit to obtain the flow field for the numerical simulation. Figure 6 shows the internal fluid model of the swirl nozzle. Figure 7 shows the internal fluid model and the external fluid model of the swirl nozzle (In Figure 7, the arrows refer to the nozzle internal fluid model shown in Figure 6).

Because the part of the nozzle core structure is complex and the diameter range is large, it is decided to divide it by unstructured grid. For external flow field model, it is decided to use structured grid to divide it, through the grid independent check, the final division results are shown in Figure 8 and Figure 9, and the total number of grid cells is 2889437.

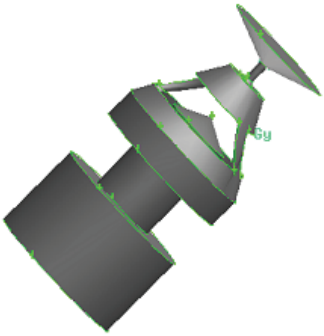

FIGURE 6. Internal flow field

FIGURE 7. Internal and external flow field

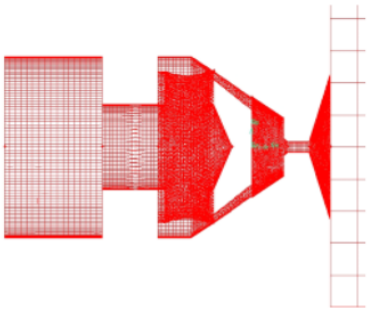

FIGURE 8. Internal flow field grid

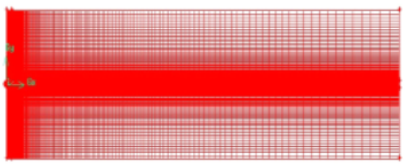

FIGURE 9. Internal and external flow field grid

4. Numerical Simulation of Swirl Nozzle and Analysis of Its Results.

4.1. **Boundary condition setting.** During the simulation, the inlet interface of the nozzle is set to the pressure-inlet boundary condition, the outflow interface is set to the pressure-outlet boundary condition, the interface between the internal flow field and the external flow field is set as the interface boundary condition, the remaining faces are set to the wall boundary condition, and the final output grid file's format is .msh.

4.2. **Swirl nozzle simulation.** The above-mentioned grid file is introduced into FLUENT and the atomization performance of the swirl nozzle is simulated. The standard k-ε turbulence model and the DPM model are selected, where the water is the continuous phase and the air is the dispersed phase. The air phase is set to 0, which means the entrance of the media is all water. In the boundary conditions, the inlet pressure is set to 0.3-1 MPa for simulation. Figures 10-13 show the simulation results of the nozzle transient droplet diameter and velocity when water pressure is equal to 0.4 MPa, 0.6 MPa, 0.8 MPa, 1 MPa.

Figure (a) shows the droplet diameter distribution in Figures 10-13. It can be seen from the figure that the droplet diameter distribution decreases as the nozzle pressure increases and the atomization angle reaches the maximum at 8 bar, but the change is relatively small. Figure (b) shows the droplet velocity distribution in Figures 10-13. It can be seen from the figure that the droplet velocity increases with pressure increasing.

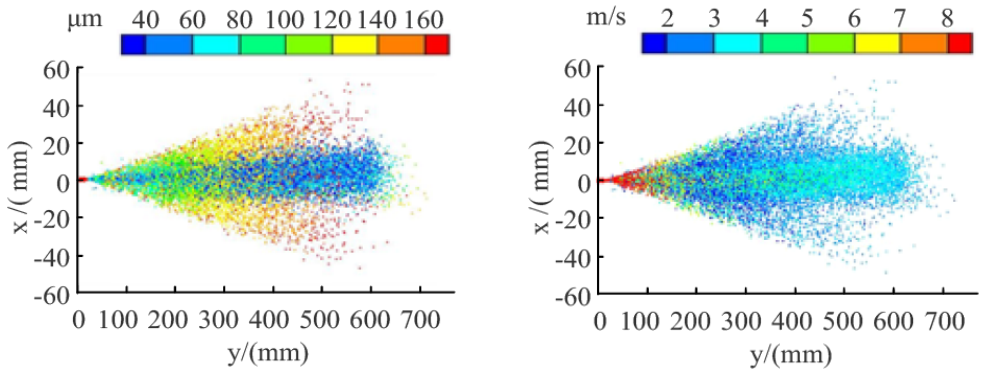

(a) Diameter distribution (b) Velocity distribution

FIGURE 10. Diameter and transient velocity distribution of droplet under the pressure of 0.4 MPa

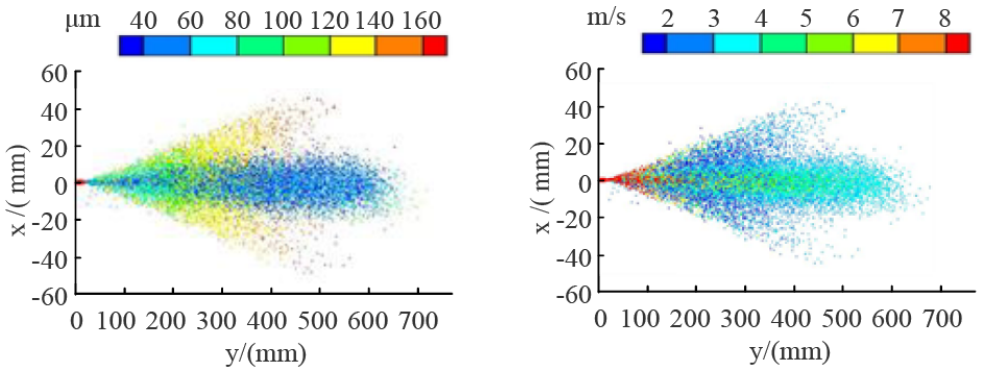

(a) Diameter distribution (b) Velocity distribution

FIGURE 11. Diameter and transient velocity distribution of droplet under the pressure of 0.6 MPa

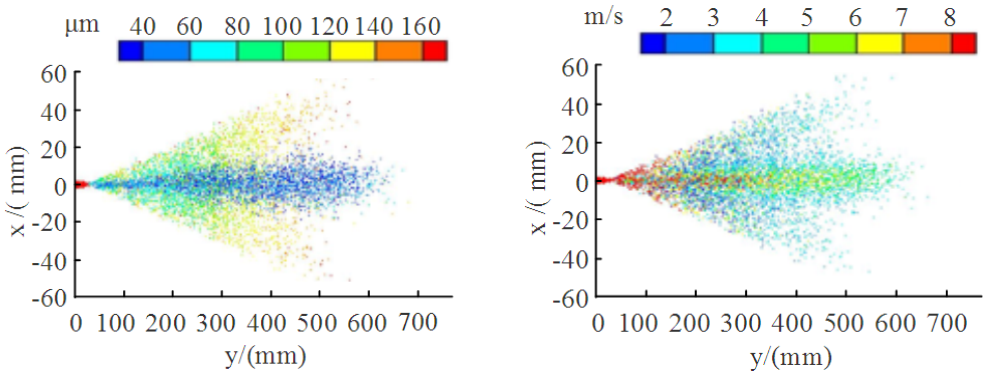

(a) Diameter distribution (b) Velocity distribution

FIGURE 12. Diameter and transient velocity distribution of droplet under the pressure of 0.8 MPa

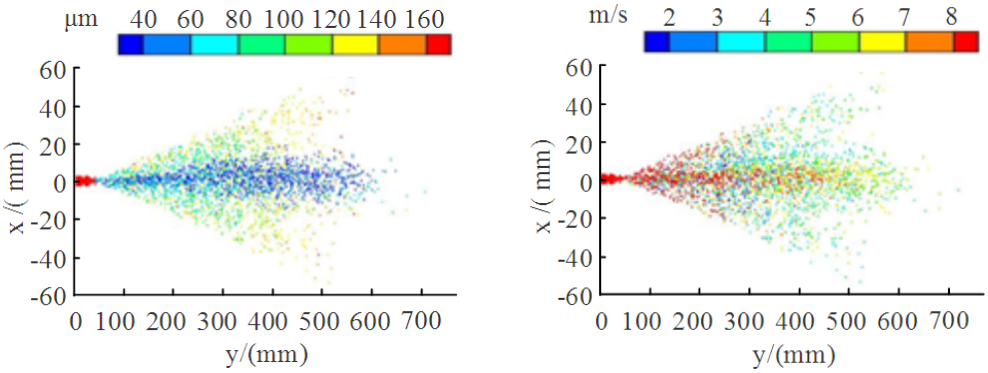

(a) Diameter distribution (b) Velocity distribution

FIGURE 13. Diameter and transient velocity distribution of droplet under the pressure of 1 MPa

The specific change value will be obtained by post-processing the atomization model in the next section.

4.3. **Analysis of numerical simulation results of atomization characteristics of swirl nozzle.** In order to visualize the simulation results, in the transient calculation process a number of 1 mm × 1 mm small cross-sections are set through the plane tab so as to capture the droplets and collect the diameter and the velocity of the droplets and other related data.

4.3.1. *Analysis of nozzle simulation results.* Figure 14 shows the position of the plane when the range is measured. The nozzle range is measured primarily by establishing a plane cross section parallel to the nozzle outlet. When the number of droplets collected in a certain period of time is less than 100, the position of the section is the farthest range of the nozzle.

As shown in Figure 15, the spray range is measured when the nozzle inlet pressure is 0.3-1 MPa. It can be seen from the analysis that with the increase of water pressure, the range of nozzle is decreasing first, the nozzle has the shortest range when the pressure is 0.8 MPa, and then the range is increasing again. At the same time, the nozzle angle increases first and then decreases, and the minimum range is generated in the vicinity of 0.8 MPa water pressure. It can be achieved through simulation that the nozzle's range is 590 mm-660 mm.

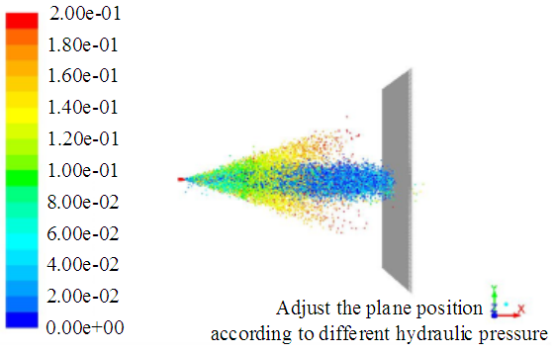

FIGURE 14. Position of the plane

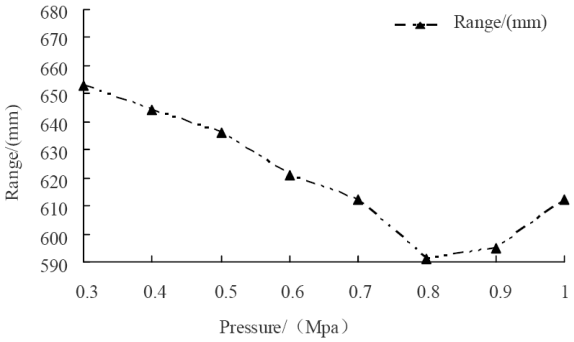

FIGURE 15. The range of spray

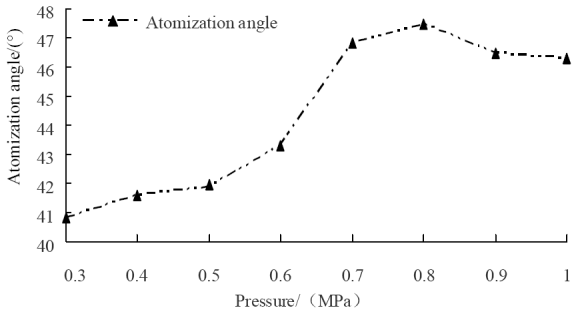

FIGURE 16. The spray angle

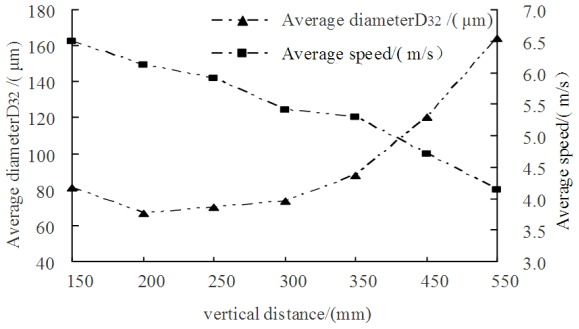

FIGURE 17. Diameter and speed under 0.6 MPa

4.3.2. *Analysis of simulation results of atomization angle.* The atomization angle measurement is mainly to save the nozzle jetting results, and then measure the nozzle atomization angle through CAXA. Figure 16 shows the change of atomization angle when the nozzle inlet pressure is 0.3-1 MPa. It can be seen that the atomization angle increases with the increase of water pressure, and the atomization angle is the largest at 0.8 MPa water pressure. With the pressure increasing, the atomization angle decreases slightly.

4.3.3. *Analysis of simulation results of atomization distribution.* Figure 17 shows the change of average diameter D_{32} and the average velocity at 150 mm, 200 mm, 250 mm, 300 mm, 350 mm, 450 mm, 550 mm different heights is simulated at 0.6 MPa water pressure. It can be seen from the figure, the droplet average diameter on 150 mm cross-section is higher than 250 mm plane, the phenomenon is mainly because of the liquid film in the crushing at the 150 mm section, which results in the cross-section of the droplet diameter irregular, but with the test plane from the nozzle outlet farther, liquid film is broken into small droplets under the surface tension and centrifugal force gradually. Due to their own gravity, small droplets also produce collisions with dust particles in the air as well as nearby drops of other droplets. So the diameter of the droplets will gradually increase, also producing the changes shown in the figure. In contrast to the change in particle diameter, the average velocity of the droplets decreases gradually as the test plane farther from the nozzle outlet. The main reason is that after the liquid film breaking, the centrifugal force of the droplet itself makes the velocity faster, but with the volume increase and the role of resistance process, the droplet velocity gradually weakened, forming a trend in the figure. In addition to the overall change in the law, we can also find from the figure at the distance from the nozzle outlet 150 mm-350 mm, the droplet average particle diameter change is relatively stable. Also at the distance from the nozzle outlet 150 mm-350 mm, the average speed change is relatively gentle. Based on the above analysis, a stable section

of the nozzle from the nozzle outlet 250 mm is chosen, and the following analysis of the distribution of the atomization will be used as a reference plane cross section.

In this case, the distribution of atomization data under the pressure of 0.4 MPa, 0.6 MPa, 0.8 MPa and 1 MPa was obtained at the plane whose distance is 250 mm. Figure 18 shows the mean diameter distribution and the average velocity distribution of the droplet at 250 mm plane from the nozzle ports at four pressures of 0.4 MPa, 0.6 MPa, 0.8 MPa and 1 MPa. According to Figure 18(a), it can be seen the average diameter of the nozzle from the center of the fog is gradually increased, but the droplet diameter increase is not much; the higher the water pressure is, the smaller the average droplet diameter is. As shown in Figure 18(b), the average velocity is subjected to a process from high to low to high, and at different pressures, the central velocities at the fog center and edge are larger, the central velocities is smaller and the higher the pressure is, the higher the velocity is.

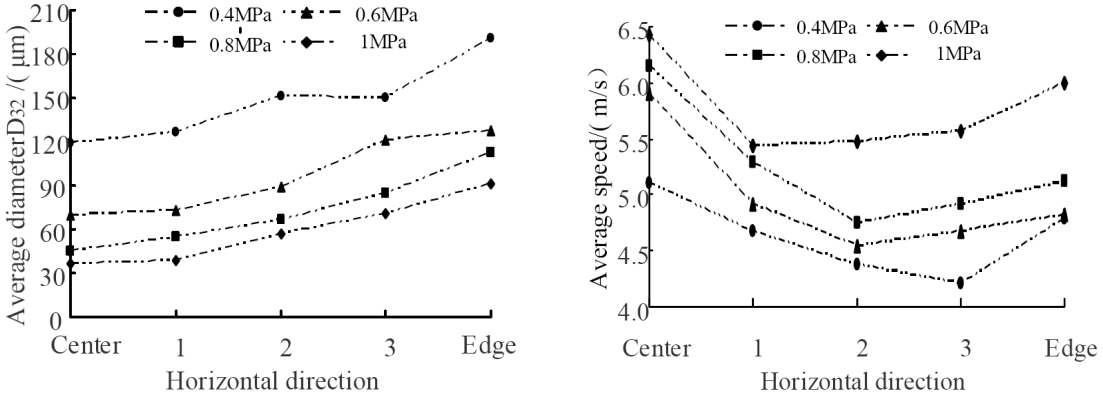

(a) Diameter distribution (b) Velocity distribution

FIGURE 18. Diameter and transient velocity distribution of droplet on the stable section

Through the simulation results, it can be seen that the atomization performance is stable under the pressure of 0.6 MPa and above 0.6 MPa. Therefore, the mean diameter distribution of droplets in different atomization sections is collected at three pressures of 0.6 MPa, 0.8 MPa and 1 MPa. Figures (a), (b) in Figures 19-21 show the average diameter and average velocity distribution of droplets in different atomization sections at 0.6 MPa, 0.8 MPa and 1 MPa. Through Figure (a) in Figures 19-21, it can be seen that the average diameter distribution of droplets decreases with increasing pressure, that is, the higher the pressure is, the smaller the diameter is. The droplet diameter distribution

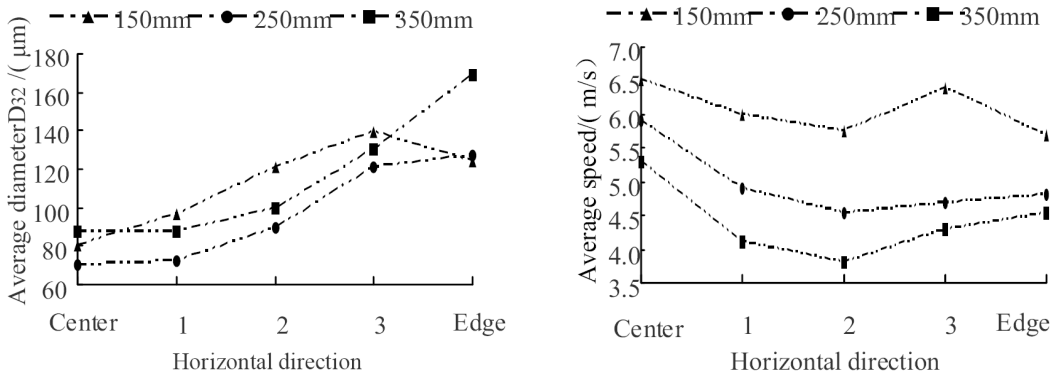

(a) Diameter distribution (b) Velocity distribution

FIGURE 19. Diameter and transient velocity distribution of droplet under different cross-section under the pressure of 0.6 MPa

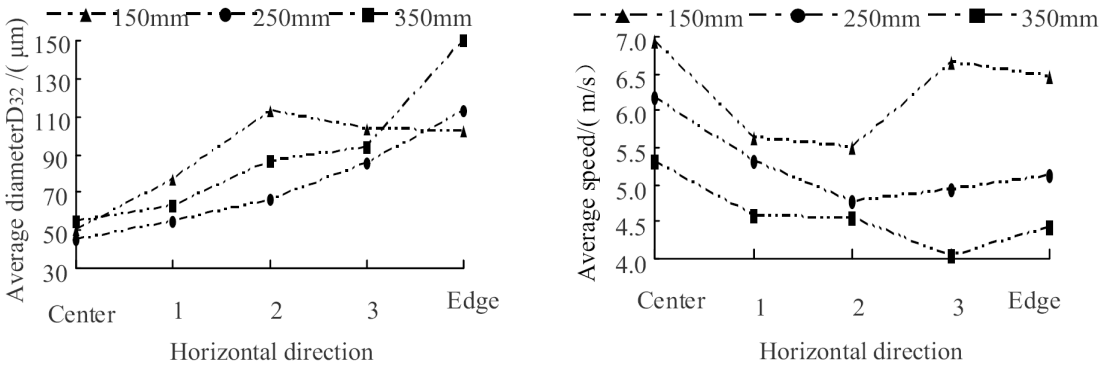

(a) Diameter distribution (b) Velocity distribution

FIGURE 20. Diameter and transient velocity distribution of droplet under different cross-section under the pressure of 0.8 MPa

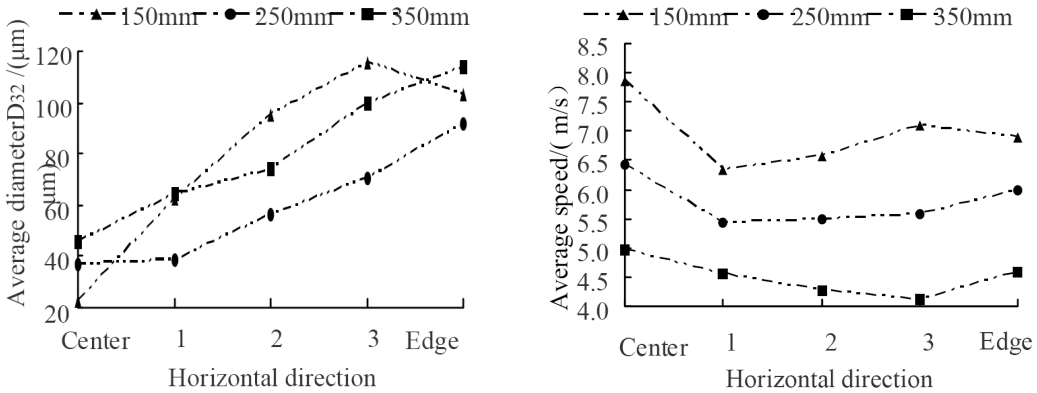

(a) Diameter distribution (b) Velocity distribution

FIGURE 21. Diameter and transient velocity distribution of droplet under different cross-section under the pressure of 1 MPa

at 150 mm cross-section is more disorderly, mainly because of its incomplete phase in the liquid film fragmentation. As shown in Figures 19-21, the droplet velocity profile shown in Figure (b) can also be seen that the liquid film is not completely broken at 150 mm, but the overall look with the pressure increases, and the nozzle of the overall droplet speed are improved.

5. **Conclusion.** The following conclusions can be drawn through the above analysis.

(1) Nozzle spray range with the increase in water pressure, shows the first to gradually reduce the range after the increase in the trend, and the minimum range is generated in the vicinity of 0.8 MPa water pressure.

(2) The atomization angle of the nozzle increases with the increase of the water pressure, and the atomization angle of the nozzle reaches the maximum at 0.8 MPa.

(3) As the pressure increases, the droplet average diameter distribution data will gradually decrease, that is, in the nozzle conditions, the higher the pressure is, the smaller the droplet diameter is. In the 0.8 MPa operating conditions, the droplet diameter of the nozzle is about 110 μm, which reaches the micron level, and the average velocity distribution of the droplet is also stable and stable.

(4) Based on the above conclusions, from the perspective of energy conservation, ensure the best atomization effect on the basis of the choice of 0.8 MPa working pressure as the best working pressure water pressure.

The above is a study on the atomization performance of the nozzle under the constant operating conditions. The main work in the future will focus on the study of nozzle atomization performance under variable conditions.

Acknowledgment. The authors would like to thank the editors and anonymous reviewers for their constructive advices greatly improving the paper.

REFERENCES

[1] S. Ma and Z. Kou, Study on efficiency of dust suppression by mist spray and its matched parameters, *China Safety Science Journal*, vol.5, pp.84-88, 2006.

[2] X. Ding, *Numerical Simulation and Structure Parameters Optimization of the Nozzle Used in Acid Regeneration System*, Master Thesis, East China University of Science and Technology, 2014.

[3] J. Li, C. Qian, B. Chen, G. Zhu, S. Zhao, T. Yan and R. Zhang, Atomization characteristics of the combined swirl feeding spray nozzle based on orthogonal design, *Chemical Industry and Engineering Progress*, vol.32, pp.985-990, 2013.

[4] J. Zhang, Y. Ren and Y. Pan, Dedusting swirl atomizing nozzle simulation and CFD flow field analysis, *Coal Mine Machinery*, vol.10, pp.47-49, 2014.

[5] G. Yang, H. Zhou and F. Liu, Simulation of flow field of high-pressure water-jet from nozzle with FLUENT, *Journal of Lanzhou University of Technology*, vol.2, pp.49-52, 2008.

[6] X. Ding, X. Wei, Q. Liu and L. Si, Study on CFD numerical simulation of atomizing nozzle colliery spray system for dust fall, *Mining & Processing Equipment*, vol.42, no.6, pp.127-131, 2014.

[7] M. Sun, *Numerical Simulation on Two-Phase Flow of Swirl Nozzle*, Master Thesis, Dalian University of Technology, 2013.

[8] Y. Xu et al., Modeling and experimental validation for truncated cone parts forming based on water jet incremental sheet metal forming, *The International Journal of Advanced Manufacturing Technology*, vol.75, nos.9-12, pp.1691-1699, 2014.

[9] D. Chatterjee, D. Mazumdar and S. P. Patil, Physical and mathematical modeling of two-phase flows in a HOLLOW JET NOZZLE, *Metallurgical and Materials Transactions*, pp.819-831, 2007.

[10] M. D. Paine, M. S. Alexander and J. P. W. Stark, Nozzle and liquid effects on the spray modes in nanoelectrospray, *Journal of Colloid and Interface Science*, 2015.